“　　—　　”

徐培全，　唐新华，　姚　舜，　俞海良

（　　　　　　　　　　　　　　　，　200030）

　　　　：　　　　　　　　　　　　　　　　　　　　　　　，

“　　—　　”　　　　　　　　　　　　　　GTAW

（MSE）　　　　　　　　　　　，　　　　　　　　　　　，

　　　　　　　，　　　　　；

　　　，　　　　　　　。

　　　：　　　　；　　　　　；　　　　　；

　　　：TG409　　　　　　：A　　　　　：0253－360X(2006)10－045－04

徐培全

0 序 言

1 焊缝 3D 计算视觉模型

　　　　　　　　　　　α,　　　　β　　　γ。　　　　　　α

　　　　　　CCD

Scheimpflug [7~8],

, Rapha L[9]

β　　　CCD

γ　　　　　　γ∈[0°~

360°),

CCD　　　　　　　　　　　3D,

图 1

、

。

图 1
Fig. 1 Projection model for 3D calculation

，，$P(x_L, y_L, z_L)$
（
） ，
$P'(x_{pixel}, y_{pixel})$，，
$P'(x_L, y_L, z_L)$
，

$$\begin{cases} x_L' = -x_c \cdot \cos\beta + l \cdot \sin\beta, \\ y_L' = -y_c, \\ z_L' = l \cdot \cos\beta + x_c \cdot \sin\beta, \end{cases} \quad (1)$$

：l

。 l'
；
$O'(l' \cdot \sin\beta, 0, l' \cdot \cos\beta)$，
，。

P，P' O'，
，PP' P'
O' $\{l\}$。

$$\frac{x - l' \cdot \sin\beta}{m} = \frac{y}{n} = \frac{z - l' \cdot \cos\beta}{p}, \quad (2)$$

：m, n, p $x、y、z$
。$s = \{m, n, p\}$，P'
O'，，P
。
，，
，
。，
x_L, y_L, z_L r

$$(x - r)^2 + y^2 = r^2。 \quad (3)$$

，。

$x_L \neq 0$

$$r = \frac{x_L{}^2 + y_L{}^2}{2x_L}。 \quad (4)$$

，

r，z_L
r_0，

$$\frac{r}{r_0} = \frac{175 - z_L}{175}。 \quad (5)$$

$$z_L = \frac{175(r_0 - r)}{r_0}。 \quad (6)$$

，$x_L = 0$，
，

$$z_L = \frac{(l' - f) \cdot \Delta}{f \cdot \sin\beta + |\Delta| \cdot \cos\beta}，\quad (7)$$

：f ；Δ
x 。

2 焊缝 3D 计算与定位结果

、 V （60°）、
，z_L γ
、3D 。，
，，$\alpha = 12°53'$，
$\beta = 39°15'$。 $25'10''$。

2.1 z_L γ

，
，。，V
580 ；
464 ； 486 ；
515 ； 544
； 400 。
z_L γ 2
。

z_L γ
，
$\gamma = \pi$ 。
2.8 mm， x_L 。

2.2 3D
" "
，3D
" — "，

图 2　z_L 与 γ

Fig. 2　Relation of depth value z_L and γ

，　　　　　　3D　　　　　　　。

　　　　　　，　　x　　　　51　　，

2 mm，　　　　　　　51　　　　　　　，

　　　　　　　　　3D　，

3　　。
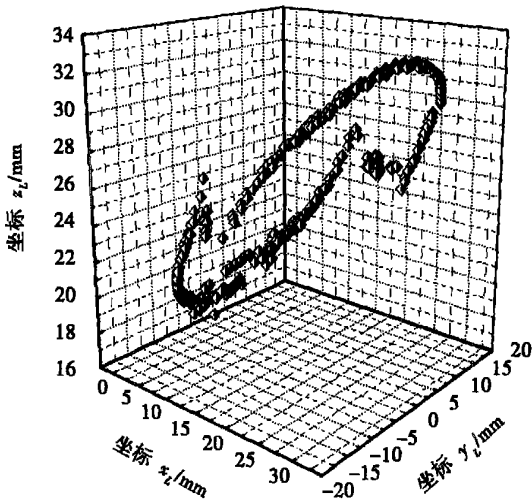
(a) 环形激光视觉传感技术

(b) 激光三角测量技术

图 3　　　　　　3D
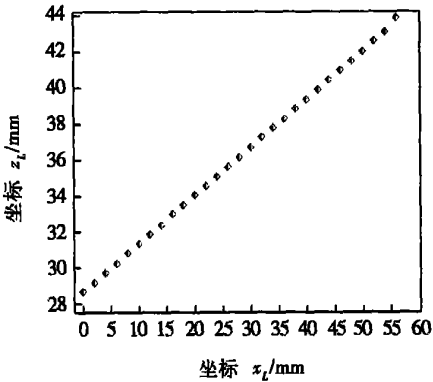
Fig. 3　Results of 3D calculation for ramp welded seam

，3D　　　　　　　MSE

。MSE

$$MSE = \frac{1}{N_t} \sum_{1}^{N_t} [z(i) - z(i)']^2 / z(i)'^2, \quad (8)$$

：$z(i)$　　　i　　　　　　　　　；$z(i)'$

　　　。　　　　，　　　　　　MSE

0.029 9，"　　　　"　　　　　　0.436 8。

　　NI1409　　　　　，　PⅢ　　　780 Hz

、　　384 M　　　　　　　　ABB—

IRB1400　　　　C/S　　　　　，　　　　、

、3D　　　　　　50 ms，　　　GTAW

　　　　　，　　　　，

、　　　，　　　　CCD　　　　　。

2. 3

　　　　　　　，

　　　　　，　4a

，　4b　　　　　　　　　，

1　　　。

(a)

(b)

图 4
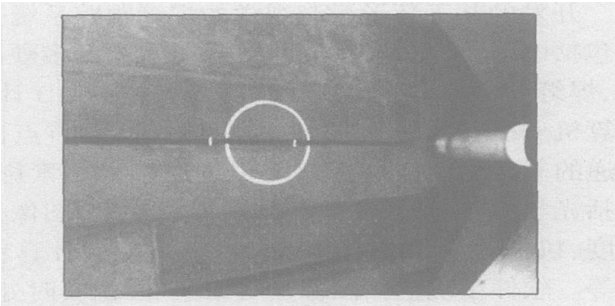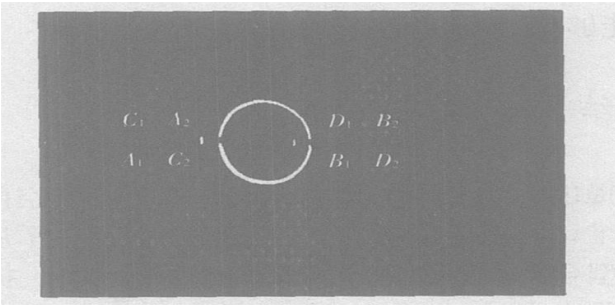
Fig. 4　Image for seam location of butt joint with gap

　　　　　　1　　　　　，　　x_L　　　　　，

　　　　　　　　0.3 mm，　　y_L　，

　　B_2　　　　　　　，

　　　　　　　。

　　　　　，　　　　　　　，

A_2　　C_2　　　　　　3.94，B_2　　D_2

　3.94。　　　　　　4 mm

1

Table 1   Comparison of seam location results

| | 3D (   ) | | | 3D (   ) | | |
	x_L	y_L	z_L	x_L'	y_L'	z_L'
A_1	39.74	2.32	0.59	40.00	3.00	0.00
A_2	38.28	−1.16	8.13	38.00	−1.00	9.00
B_1	0.01	0.69	−0.69	0.00	2.00	0.00
B_2	0.11	−2.09	7.04	0.00	−2.00	9.00
C_1	39.85	−0.46	0.72	40.00	−1.00	0.00
C_2	38.15	2.78	7.97	38.00	3.00	9.00
D_1	0.05	−1.39	−0.64	0.00	−2.00	0.00
D_2	0.11	1.86	7.01	0.00	2.00	9.00

0.06 mm。 z_L , x_L, y_L
,   0.59,
0.87, 0.69, 1.96, 0.72, 1.03, 0.64   1.99 mm。

z_L x_L、y_L

、   、   3D   、

—   ,

,   ,

,   、

、   3D

。   、   、

、   C/S

,   。

4   结   论

,

、   ,   C++

:

[1]   ,   .   [M] .   :

. 2006

[2]   Hsing C K, Li J W. An image tracking system for welded seams using fuzzy logic[J] . Journal of Materials Processing Technology, 2002, 120 (1−3): 169−185.

[3]   Ushio M, Mao W. Sensors arc weld[J] . Adv. Limitation, 1994, 23: 135−141.

[4]   Tsao T R, Chen V C. Gabor wavelet pyramid for depth recovery[J] . Proceedings of SPIE-The International Society for Optical Engineering, 1994, 2242: 161−168.

[5]   Rajagopalan A N, Chaudhuri S, Chellappa R. Quantitative analysis of error bounds in the recovery of depth from defocused images[J] . Journal of the Optical Society of America; Optics and Image Science, and Vision, 2000, 17(10): 1722−1731.

[6]   Lee S K, Na S J. A study on automatic seam tracking in pulsed laser edge welding by using a vision sensor without an auxiliary light [J] . Journal of Manufacturing Systems, 2002, 21 (4): 302−315.

[7]   Porta J M, Verbeek J J, Krose B J. Active appearance based robot localization using stereo vision[J] . Auton Robot, 2005, 18 (1): 59−80.

[8]   Bae K Y, Lee T H, Ahn K C. An optical sensing system for seam tracking and weld pool control in gas metal arc welding of steel pipe [J] . Journal of Materials Processing Technology, 2002, 120(1−3): 458−465.

[9]   Wu M S. Konzeption und realisierung optischer sensorsysteme zur nahtfuehrung und parameter adaption beim lichtbogenschweissen[D] . Germany: RWTH Aachen, 1993

[10]   ,   ,   .
                [P]   : CN1715989.

:   , , 1978   10   ,   。
、   ,   4 。

Email: xupeiquan7810@yahoo.com. cn

welding of aluminum alloy. The experiment results demonstrate that the addition of the metal powder enhances the energy coupling efficiency and reduces the power density threshold value during laser deep welding. Such as the reducing rate is about 50% for A2219 alloy. The experiment results also indicate that the powder can enter the weld pool availably only the powder was delivened to the suitable area after laser beam at the surface of a part. The proper quantity of the alloy powder must match with the right power density and energy input, which can assure to obtain good weld appearance. Meanwhile, the addition of the powder can reduce the fluctuation of the laser-induced plasma and maintain its stability effectively in the laser welding. So a stable welding process and good weld appearance can be obtained in the experiments.

Key words: aluminum alloy; metal powder; CO_2 laser welding; laser-induced plasma; power density threshold value

Effect of side gas on laser induced plasma during laser deep penetration welding

ZHANG Lin-jie[1], ZHANG Jian-xun[1], DUAN Ai-qin[2] (1. State Key Laboratory of Mechanical Behavior for Materials, Xi'an Jiaotong University, Xi'an 710049, China; 2. Beijing Aeronautical Manufacturing Technology Research Institute, Beijing 100024, China). p37—40

Abstract: A two dimensional compressible gas flow model of laser penetretion welding process was founded for a better understanding of the influence of side gas flow conditions on the behavior of laser induced plasma. The distributions of temperature and velocity within plasma plume under different side gas flow conditions were calculated. The shape and size of plasma in laser welding process was studied with high-speed CCD camera. The result shows that laser induced plasma and weld geometry are sensitive to side nozzle height, its inclination angle and side gas flow rate; that cooling effect and assist-gas/plasma-plume momentum ration play an important role in controlling the plasma plume.

Key words: laser deep penatration welding; side assist gas; numerical simulation; high-speed CCD imaging

Mechanical properties and microstructures of QFP micro-joints soldered with diode-laser soldering system

HAN Zong-jie, XUE Song-bai, WANG Jian-xin, CHEN Xu (College of Materials Science and Technology, Nanjing University of Aeronautics and Astronautics, Nanjing 210016, China). p41—44

Abstract: Soldering experiments of two kinds of devices QFP32 and QFP48 were carried out using diode-laser soldering system and IR reflow soldering method, and the distribution regulations of the tensile strength of QFP micro-joints with Sn-Pb solder and Sn-Ag-Cu lead-free solder were studied by STR-1000 micro-joints tester, and the characteristics of fracture microstructures of micro-joints were also analyzed by SEM. The results indicate that tensile strength of QFP micro-joints soldered with laser soldering system is larger than that with IR reflow soldering method, and tensile strength of QFP48 micro-joints is larger than that of QFP32 micro-joints. Fracture mechanism of micro-joints soldered with laser soldering system is toughness fracture, while fracture mechanism of micro-joints soldered with IR reflow soldering method includes brittle fracture and toughness fracture.

Key words: diode-laser soldering; QFP devices; mechanical properties of micro-joints; microstructures

Active vision sensing method for weld location by " circle-depth relation" algorithm

XU Pei-quan, TANG Xin-hua, LU Jian-bo, Yao Shun (School of Material Science and Engineering, Shanghai Jiaotong University, Shanghai 200030, China). p45—48

Abstract: Three vital angles were put forward, so the weld could be described by three-dimensional information. On this basis, mathematical model of depth recovery according to "circle-depth relation" algorithm and projection rules was constructed. The relation ship between depth values and off-axis angle γ under gas tungsten arc welding experiment condition was addressed by real experiment and the characteristic points of weld was described and located. Mean square error was used to analyze the recovery precision. The results showed: (1) Depth recovery for butt joint and ramp welded seams realized; (2) Weld can be located very well by using proposed vision sensor based on circular laser trajectory; and proposed vision sensor manifested a promising result with high precision and high efficiency.

Key words: laser cone projection; circular laser trajectory; depth recovery; seam location

Instantaneous energy waveform of short circuiting transition in CO_2 arc welding

XUE Jia-xiang, YANG Guo-hua, WANG Zhen-min, LIU Xiao, HONG Sen (College of Mechanical Engineering, South China University of Technology, Guangzhou 510640, China). p49—52, 84

Abstract: The welding process of three arc welding machines had been tested and analyzed with the welding dynamic arc wavelet analyzer developed by the anthers. The experimental results indicate that the instantaneous energy can synthetically reflect the influence of current and voltage on dynamic arc characteristics. To make arc ignite successfully, the instantaneous energy should increase to enough high quickly along with the current. In a cycle of short circuting transition during the steady welding process, the instantaneous energy during arc burning should be kept at the constant base, and then it falls to smaller value rapidly, finally, it rises rapidly and completes the short circuit transition. The instantaneous energy falls again rapidly to base after arc re-striking. While arc extinguishing, the instantaneous energy falls slowly to zero and avoids serious impulsion. The experiment results can provide for the foundation to design and control accurately the waveform of the welding current and voltage.

Key words: instantaneous energy; wavelet analysis; repeatability of waveform

Effects of temperature and coatings on wettability of Sn-Cu-Ni lead-free solder

WANG Jian-xin[1], XUE Song-bai[1], HAN Zong-jie[1], WANG ning[1], YU Sheng-lin[2] (1. College of Materials Science and Technology, Nanjing University of Aeronautics and Astro-